# Structured Light System for Underwater Inspection Operations

Flávio Lopes, Hugo Silva, José Miguel Almeida, Alfredo Martins, Eduardo Silva

INESC TEC Institute for Systems and Computer Engineering of Porto
ISEP - School of Engineering, Porto Polytechnic Institute, Porto, Portugal
Email: fmlopes, hugo.m.silva, jose.m.almeida, aom, eduardo.silva @inesctec.pt

***Abstract*—In this work we propose the development of a stereo SLS system for underwater inspection operations. We demonstrate how to perform a SLS calibration both in dry and underwater environments using two different methods. The proposed methodology is able to achieve quite accurate results, lower than 1 mm in dry environments. We also display a 3D underwater scan of a known object size, a sea scallop, where the system is able to perform a scan with a global error lower than 2% of the object size.**

***Keywords*—Underwater vision system, Camera, Line laser, Structured light system.***

## I. Introduction

Underwater exploration has been in the forefront of robotics community research goals. Robots deep sea exploring is crucial to most prominent underwater based industries such as oil and gas and underwater mining. Already in recent years, robotics community has been putting a significant amount of effort into the development of novel sensing and perception mechanisms to conduct underwater world exploration.

In this paper we address this issue by developing a novel low-cost structured light system (SLS) for conducting perception tasks in underwater operations. The use of pure visual perception methods is limited in underwater environments due to issues like e.g. low illumination conditions, not enough image texture and also water disturbances such as turbidity, absorption and scattering [1]. It is difficult to obtain accurate 3D information using conventional computer vision approaches such as stereoscopic vision due to limitations in obtaining images point correspondences. One way of overcoming such limitation is by using laser based techniques [2], or laser techniques combined with photometric stereo [3]. In [4] structured light systems are used to perform bathymetric surveys using Remotely Operational Vehicles and discoverer diffuse flow on the seabed.

One of the main issues that has a very high impact in the results obtained by the SLS system, is its calibration. Which must conducted in an efficient manner and using a procedure able to calibrate (obtain parameters) allowing to relate the laser line in the camera reference frame, and thus perform the SLS calibration. The problem of calibrating a triangulation system between a laser (projector) and a camera has already been addressed in previous research, but the idea is still subject of ongoing research especially when trying to apply it for underwater operations. In [5] a calibration rig consisting of lines with known parameters is used. The intersection of the laser plane with each line gives an image point to world line correspondence. Having enough correspondences a $4 \times 3$ transformation matrix which maps a 2D image point to its 3D coordinate on the laser plane can be recovered.

In this work we present two possible methods for calibrating the SLS system, one of them is modified version on the method developed by Huynh [6]. The method uses a calibration rig consisting of two planes with 12 points (control points) with known 3D coordinates. The points form 4 straight lines, and by using the cross-ratio invariance [7] , the 3D coordinates of the point of intersection of the laser plane with these 4 lines can be determined, allowing to obtain 2D image point to 3D world point correspondences that are used to recover the transformation matrix. Some methods are far complex and other simpler methods that require just a few measurements to a known planar target from different viewpoints can also be used to compute the camera and projector calibration [8], [9]. Where an image of the calibration board is captured, along with the line of its intersection with the laser plane, by obtaining correspondences between chessboard points and their image coordinates, the pose of the calibration board with respect to the camera center can be determined, resulting in a known world plane. The image of the laser line is then back-projected to the world plane. Performing this operations with the calibration board at different orientations results in a 3D point cloud spanning the laser plane, from which the parameters that define the laser plane can be recovered.

The SLS calibration is only part of the problem to solve, and there are many possible applications for this type of system that were already explored by other authors. In [10] 3D reconstruction method based on the laser line scan (LLS) system, for the purpose of underwater surveying. The LLS systems can be mounted, on a ROV for conducting underwater surveys and create high resolution bathymetric maps. C. Roman et al.[11] used a structured light laser profile imaging to create high resolution bathymetric maps of underwater archaeological sites. The work evaluate laser profile imaging in comparison to stereo imaging and high frequency multi-beam mapping, and results show very promising resolution in comparison to multi-beam and stereo reconstructions, particularly in low contrast scenes.

Contrary to other SLS systems that are designed for a specific task, our system tends to be a general purpose system for industry underwater applications with the capability of also being used as an add-on sensor for performing structures mapping surveys using underwater and surface vehicles. To do so, we develop and propose two different methods of performing SLS calibration capable of being applied in dry and underwater environments, and also present results of 3D mapping information in both operational environments.

This paper is organized as follows: in chapter II the geometric model of SLS system is presented. In chapter III the two SLS calibration methods are presented in detail. In chapter IV we present the calibration results for the two calibration procedures in both dry and underwater environments, and also present some results of the obtained point cloud using different objects in these scenarios. Finally in chapter V conclusions and some of our future work is presented.

## II. Geometric Model

Our SLS system is composed of a camera and two line lasers (projectors) equipped with a line beam. The main objective is to be able to obtain accurate 3D points information from objects that are illuminated by the projectors. The geometric model of the SLS system is displayed in Fig.1, where we can see the projection plane for one of the projectors in camera coordinates.

### A. Camera Model

The camera model follows a classic pinhole model of perspective projection divided into intrinsic(1) and extrinsic parameters.

$$K = \begin{bmatrix} f_x & s & c_x \\ 0 & f_y & c_y \\ 0 & 0 & 1 \end{bmatrix} \tag{1}$$

where $K$ is the intrinsic parameter matrix, that contains the focal length $\mathbf{f}$ $(f_x,\ f_y)$, the skew $s$, and the principal point $\mathbf{c}$ $(c_x, c_y)$ information. There is still one parameter missing which is the lenses distortion that needs to be compensated when calibrating the camera [12].

What concerns the extrinsic parameters, the projection of a 3D world point $\mathbf{P}_w$ represented in the world coordinate system to a 2D image point $\mathbf{p}$ (x,y), in the image plane is given by :

$$\tilde{\mathbf{p}} \simeq K[R|\mathbf{t}]\tilde{\mathbf{P}}_\mathbf{w} \tag{2}$$

where $R$ is the rotation matrix, $K$ the intrinsic parameters and $\mathbf{t}$ the translation vector that allows to translate a point between the world reference frame and the camera reference frame. While $\tilde{\mathbf{p}}$ is a 2D image point and $\tilde{\mathbf{P}}_\mathbf{w}$ is the same point in the 3D world point reference frame, both in homogeneous coordinates representation.

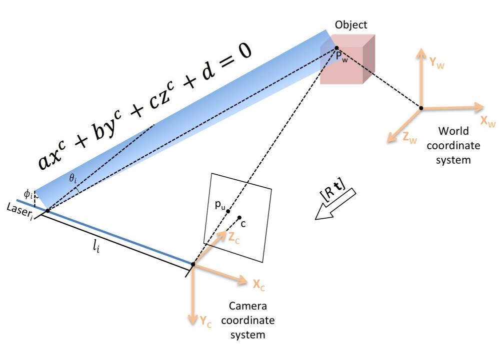


Fig. 1. Geometric model of the SLS system

### B. Projector Model

For the projector calibration, the perspective projection does not hold since the light stripe is not directly illuminated from the optical center of the projector. Therefore, most applications do not use the projection of the light stripe, and instead prefer to represent the projector with the equation of a plane. One assumes that the calibration of each light projector is conducted completely independent. The light stripe that appears in 3D space can be expressed in the camera coordinate frame by the plane equation, described by:

$$a_i x_c + b_i y_c + c_i z_c + d = 0 \tag{3}$$

where $i$ is the light stripe number, $a_i, b_i, c_i$, and $d_i$ are its coefficients. From here, it is possible to define the baseline $l_i$ i.e the distance between the camera and the projector, and also the projection angle $\theta_i$ i.e the angle between the light stripe and the $Z_c$ axis, and the tilt angle $\phi_i$ i.e the angle between the $Y_c$ axis and the light stripe. The parameters can be given by:

$$l_i = \left(\frac{d_i}{a_i}\right) \tag{4}$$

$$\theta_i = \arctan\left(\frac{-ci}{a_i}\right) \tag{5}$$

$$\phi_i = \arctan\left(\frac{-b_i}{a_i}\right) \tag{6}$$

### C. Triangulation

For obtaining the 3D world point information $\mathbf{P_w}$ in the camera reference frame as $\mathbf{P_c}$ $(x_c, y_c, z_c)$, a triangulation principle between the camera viewpoint and the light stripe is used. To do so, the camera and projector parameters are derived from (2) and (3), as given by:

$$\begin{bmatrix} f_x & s & 0 \\ 0 & f_y & 0 \\ a_i & b_i & d_i \end{bmatrix} \begin{bmatrix} \frac{x_c}{z_c} \\ \frac{y_c}{z_c} \\ \frac{1}{z_c} \end{bmatrix} = \begin{bmatrix} x - c_x \\ y - c_y \\ -c_i \end{bmatrix} \tag{7}$$

So, we can estimate $\mathbf{P_c}$ coordinates as:

$$x_c = \frac{x - c_x}{f_x} z_c \tag{8}$$

$$y_c = \frac{y - c_y}{f_y} z_c \tag{9}$$

$$z_c = \frac{l_i}{-\frac{c_i}{a_i} - \left(\frac{x-c_x}{f_x}\right) - \frac{b_i}{a_i}\left(\frac{y-c_y}{f_y}\right)} \tag{10}$$

The triangulation principle is used to compute the depth coordinate $z_c$ (10). Afterwards we can obtain the $x_c$, $y_c$ coordinates based on the scaling relation with the camera (8) (9), considering skew $s = 0$.

## III. Calibration

Prior to be able to use the structured light system for obtaining accurate 3D underwater measurements, there is the need to perform a global system calibration. We need to calibrate the camera (intrinsic and extrinsic parameters), and each projector position with respect to the image plane.

### A. Camera Calibration

The first step to obtain a global system calibration is to recover all camera parameters. Therefore, we start by obtaining the camera intrinsic parameters by using an offline toolbox procedure.

Afterwards camera extrinsic parameters are obtained by taking at least two images of a plain chessboard in different viewpoints, then all chessboard corners present in each image are detected using the Harris corners detector [13]. The extrinsic parameters (rotation matrix $R$, translation vector $\mathbf{t}$) are recovered based on homography decomposition method [9].

We establish that 3D world points in the world reference frame have null component in $Z_w$ axis, i.e, all the selected points have $z_w = 0$. These points can be represented in homogeneous coordinates by equation (11). The 2D points in image plane without distortion, can be represented in homogeneous coordinates by equation (12).

$$\tilde{\mathbf{P}}_\mathbf{w} = \begin{bmatrix} x_w \\ y_w \\ 0 \\ 1 \end{bmatrix} \tag{11}$$

$$\tilde{\mathbf{P}}_\mathbf{u} = \begin{bmatrix} u \\ v \\ 1 \end{bmatrix} \tag{12}$$

To define the set of points, $\tilde{\mathbf{P}}_\mathbf{u}$ and $\tilde{\mathbf{P}}_\mathbf{w}$, all corners of the chessboard are used. Therefore, it is possible to relate a world point $\tilde{\mathbf{P}}_\mathbf{w}$ and its image correspondent $\tilde{\mathbf{P}}_\mathbf{u}$ up to a unknown scale $\lambda$ by means of homography *H* as given by:

$$\lambda \tilde{\mathbf{P}}_\mathbf{u} = H \tilde{\mathbf{P}}_\mathbf{w} \tag{13}$$

To obtain the rotation matrix $R$ and translation vector $\mathbf{t}$ is necessary to perform homography $H$ decomposition by:

$$H = K\left[\mathbf{r_1} \quad \mathbf{r_2} \quad \mathbf{t}\right] = \left[\mathbf{h_1} \quad \mathbf{h_2} \quad \mathbf{h_3}\right] \tag{14}$$

With the intrinsic parameters known, the transformation from world to the camera coordinate frame can be obtained by:

$$\begin{cases} \mathbf{r_1} = \lambda_1 K^{-1}\mathbf{h_1} \\ \mathbf{r_2} = \lambda_2 K^{-1}\mathbf{h_2} \\ \mathbf{r_3} = \mathbf{r_1} \times \mathbf{r_2} \\ \mathbf{t} = \lambda_3 K^{-1}\mathbf{h_3} \end{cases} \tag{15}$$

With:

$$\begin{cases} \lambda_1 = \frac{1}{||A^{-1}h_1||} \\ \lambda_2 = \frac{1}{||A^{-1}h_2||} \\ \lambda_3 = \frac{\lambda_1 + \lambda_2}{2} \end{cases} \tag{16}$$

Thus, the rotation matrix relating the world coordinate system to the camera coordinate system is described by:

$$R_{\text{temp}} = \left[\mathbf{r_1} \quad \mathbf{r_2} \quad \mathbf{r_3}\right] \tag{17}$$

Since the matrix $R_{temp}$ does not satisfy the orthonormality constraint of a standard rotation matrix. It is necessary to normalize and orthonormalize the matrix, using the SVD (Singular Value Decomposition) by:

$$R = UW'V^{\mathrm{T}} \tag{18}$$

Where the matrix *W'* is:

$$W' = \begin{bmatrix} 1 & 0 & 0 \\ 0 & 1 & 0 \\ 0 & 0 & ||UV'|| \end{bmatrix} \tag{19}$$

With the calculation of the matrix *R* and the translation vector $\mathbf{t}$ is possible define the position of the optical center of the camera relative to the world reference, thus completing the extrinsic parameters calibration.

### B. Projector Calibration

For the projector calibration we implemented two different methods that are describe in detail in the following sections. The first method denoted as **SLSC-CR** is based on the cross-ratio invariance principle. While the second method denoted as **SLSC-LP** is based on the robust fitting of the laser line projection. Both methods allows us to obtain control points belonging to the light stripe. Afterwards, by non-linear least squares fitting is possible to define the equation of the plane in the camera coordinate frame using $n$ control points of two different images taken in different viewpoints. Thus, by equation (20) is possible to determine each axis component $(a, b, c, d)$:

$$d_i = \frac{|ax_c + by_c + cz_c + d|}{(a^2 + b^2 + c^2)^{\frac{1}{2}}} \tag{20}$$

where $x_c, y_c, z_c$ are the control points coordinates in the camera reference frame.

### C. SLSC-CR Method

The objective for the projector calibration is to discover the equation of the plane that describes the projector light stripe in the camera reference frame.

Our first implementation **SLSC-CR** (Structured Light System Calibration - Cross-Ratio), allows to calculate the relationship between a set of a collinear points belonging to the same line. This relationship is invariant under projective transformation, and helps relate known laser points in the image reference frame with the laser points correspondences in the world reference frame.

The relationship used to establish the cross-ratio is displayed in Fig.2. It contains the 3D camera coordinate frame with four collinear points (*a,q,c,d*) and 3D world coordinate frame defined on the calibration target with points (*A,Q,C,D*).

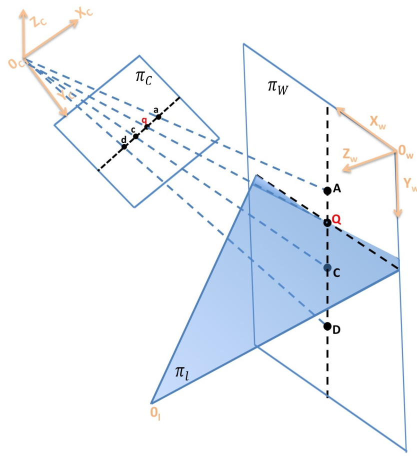


Fig. 2. Control points used to calculate the cross-ratio.

The plane $\pi_C$ defines the camera plane, plane $\pi_W$ is the calibration target plane and $\pi_l$ is the projector plane.

We start the method implementation, using a set of points in image coordinates for each horizontal line of the planar chessboard.

The following procedure was defined:

- $a_i$ and $d_i$ - corners of the right and left side of the chessboard.
- $b_i$ or $c_i$ - middle corner of the chessboard (the definition of this point depends of the $q_i$ point position)
- $q_i$ - intersection point between the projector plane and target horizontal line.

For computing the cross-ratio is necessary to preserve the correct order of selected points. Therefore, we considered two different situations for the projector line points, i.e, when the projector focus on the right side or left side of the calibration plane. In Fig.3 is possible to see the control point selection in both cases.

Afterwards, the value of the cross-ratios using 4 collinear points in image plane, can be defined as $\mathrm{CR_i}$. As the value of cross-ratio is invariant, the value of $\mathrm{CR}_i$ in world plane is the same. So, we can calculate the equation (21) in order to control point $Q$, as given by (when the projector focus on the left side):

$$
\begin{aligned}
CR_\mathrm{i} &= \frac{(A_\mathrm{i}-C_\mathrm{i})(Q_\mathrm{i}-D_\mathrm{i})}{(A_\mathrm{i}-D_\mathrm{i})(Q_\mathrm{i}-C_\mathrm{i})} \iff \\
Q_\mathrm{i} &= \frac{-A_\mathrm{i}D_\mathrm{i}+C_\mathrm{i}D_\mathrm{i}+A_\mathrm{i}C_\mathrm{i}CR_\mathrm{i}-C_\mathrm{i}D_\mathrm{i}CR_\mathrm{i}}{A_\mathrm{i}CR_\mathrm{i}-D_\mathrm{i}CR_\mathrm{i}-A_\mathrm{i}+C_\mathrm{i}}
\end{aligned} \tag{21}
$$

When the projector focus in the right side, a similar procedure can be used.

In our calibration procedure, we considered 6 control points in each image, and the control points in world coordinates are computed using their corresponding camera coordinates.

Fig. 3. Point selection based on light stripe chessboard position

.

### D. SLSC-LP Method

Our second implementation **SLSC-LP** (Structured Light System Calibration - Line Projection) allows us to increase the control points that define the projector plane. With 2D image points that belong to the light stripe and camera calibration parameters is possible obtain the points 3D coordinates. We use the projective equation and assuming that $z_w = 0$ to calculate the points in world frame ($x_w$, $y_w$), as described by:

$$
\begin{bmatrix} P_u \\ P_v \\ 1 \end{bmatrix} = K[R \quad | \, \mathbf{t}] \begin{bmatrix} x_w \\ y_w \\ z_w \\ 1 \end{bmatrix} \iff \tag{22}
$$

$$
\begin{bmatrix} P_u \\ P_v \\ 1 \end{bmatrix} = \begin{bmatrix} f_\mathrm{x} & 0 & c_\mathrm{x} \\ 0 & f_\mathrm{y} & c_\mathrm{y} \\ 0 & 0 & 1 \end{bmatrix} \begin{bmatrix} R_{11} & R_{12} & R_{13} & t_x \\ R_{21} & R_{22} & R_{23} & t_y \\ R_{31} & R_{32} & R_{33} & t_z \end{bmatrix} \begin{bmatrix} x_w \\ y_w \\ z_w \\ 1 \end{bmatrix}
$$

$$
\begin{cases}
x_w \overbrace{(P_{x'}R_{31} - R_{11})}^{\mathrm{a1}} + y_w \overbrace{(P_{x'}R_{32} - R_{12})}^{\mathrm{b1}} = \overbrace{(P_{x'}t_z + t_x)}^{\mathrm{c1}} \\
x_w \underbrace{(P_{y'}R_{31} - R_{21})}_{\mathrm{a2}} + y_w \underbrace{(P_{y'}R_{32} - R_{22})}_{\mathrm{b2}} = \underbrace{(P_{y'}t_z + t_y)}_{\mathrm{c2}}
\end{cases} \tag{23}
$$

$$
\begin{cases}
(b_2a_1 - b_1a_2)x_w = (b_2c_1 - b_1c_2) \iff x_w = \dfrac{(b_2c_1 - b_1c_2)}{(b_2a_1 - b_1a_2)} \\
(a_2b_1 - a_1b_2)y_w = (a_2c_1 - a_1c_2) \iff y_w = \dfrac{(a_2c_1 - a_1c_2)}{(a_2b_1 - a_1b_2)}
\end{cases} \tag{24}
$$

$$
P_{x'} = \frac{P_u - c_x}{f_x} \qquad P_{y'} = \frac{P_v - c_y}{f_y} \tag{25}
$$

## IV. Experimental Results

In this section, we present results for both calibration methods with experimental evaluation in dry and underwater environments. Furthermore, 3D scans of known objects size were also performed in order to validate the system.

Fig. 4. Structured Light System experimental setup consisting on two line lasers configuration, one green and one red laser on each side and a SXGA Basler camera in the middle.

## A. *Experimental setup*

Our experimental setup is composed by a red line laser beam with 635 nm wavelength, a green line laser beam 532 nm wavelength and a camera with SXGA resolution, coupled together in a water proof casings with 10 cm baseline, as illustrated in Fig.4. We use two lasers with different wavelength in order to understand the wavelength influence in the performed experiments. Our calibration procedures were implemented in MATLAB as a proof concept.

## B. *Calibration accuracy*

In order to validate the calibration, we compare both methods results with the results we obtain using known 6 points 3D information (world coordinates) obtained using the camera sensor model with 2D image information by applying the cross-ratio invariance. This can be considered a weak ground-truth system. In future work, we plan to use a LIDAR system that can map the real position of the planar chessboard and compare the results of both implementations with a more accurate 3D LIDAR information.

For obtaining these results, a set of more than 100 points including at least 6 control points in each image were utilized. In Fig.5 is possible to see the calibration process setup. During calibration, the planar target was at different depth distances that vary between 20 cm and 1.5 m.

The results presented in Table I, show that **SLSC-LP** method performs more accurately in an dry environment compared with the **SLSC-CR** cross-ratio method with over 30% improvement, it is important to mention that for the red laser results the **SLSC-LP** method has an overall RMS error lower than 1 mm. The same experiment was performed in underwater environment, see Table III. We can state that both methods accumulate about 2x more error in underwater environment. We can also see that the red laser exhibits a lower error for both method implementations in dry and underwater environments.

## C. *3D Scan*

After having evaluated the calibration results, we tested our SLS system by performing 3D Scans of known objects (work-pieces) in underwater enviroments and comparing the 3D Scan results with the object size.

Fig. 5. Calibration Setup, experiments performed in different underwater tanks at various underwater depths .

TABLE I. RMS Error Comparison between **SLSC-CR** and **SLSC-LP** in dry environments

| Lasers | Methods | x (mm) | y (mm) | z (mm) | xyz (mm) |
|---|---|---|---|---|---|
| Red | SLSC-CR | 0.0894 | 0.1215 | 0.9847 | 1.1062 |
| | SLSC-LP | 0.0390 | 0.0990 | 0.6424 | 0.7804 |
| Green | SLSC-CR | 0.3210 | 0.4421 | 1.1840 | 1.9471 |
| | SLSC-LP | 0.1852 | 0.2141 | 0.9943 | 1.3936 |

TABLE II. RMS Error Comparison between **SLSC-CR** and **SLSC-LP** in underwater environments

| Lasers | Methods | x (mm) | y (mm) | z (mm) | xyz (mm) |
|---|---|---|---|---|---|
| Red | SLSC-CR | 0.3421 | 0.6231 | 1.4330 | 2.3982 |
| | SLSC-LP | 0.2698 | 0.4488 | 1.2330 | 1.9516 |
| Green | SLSC-CR | 0.6122 | 0.4136 | 1.4213 | 2.4471 |
| | SLSC-LP | 0.3662 | 0.4573 | 1.3671 | 2.1906 |

TABLE III. Comparison between the scallop known size and 3D scan measurements

| Pose | Feature | True Value (mm) | Measured Value (mm) | Relative Error (%) |
|---|---|---|---|---|
| 0 | $L_1$ | 61.28 | 61.06 | 0.3590 |
| 0 | $L_2$ | 111.46 | 112.42 | 0.8613 |
| 0 | $L_3$ | 10.82 | 10.90 | 0.7394 |
| 1 | $D_1$ | 103.12 | 100.87 | 2.1819 |
| 1 | $D_2$ | 21.44 | 21.02 | 1.9590 |
| 2 | $H_1$ | 22.28 | 22.72 | 1.9749 |

To perform the 3D scan we coupled the SLS system to a moving platform and the objects were placed in front of the tank for the scan. As an example we can see in Fig.6, a scallop which was one of the scanned objects. In Fig.7, a 3D point cloud of the scallop generated by the SLS system when performing the scan is displayed. The moving platform has motion system with wheel encoders that provided odometry information to construct the scallop 3D representation. Measures of known size are displayed in Fig.8, and in table III we can see the results comparison between the 3D scan and the known measured values.

# V. Conclusions and Future work

In this paper we have presented two methods for calibrating a SLS system for perception in dry or underwater environments. The results comparison of both methods in dry and underwater experiments showed that the LP method has lower root means square error both in dry and underwater scenario. A

Fig. 6. Scanned object - scallop

.

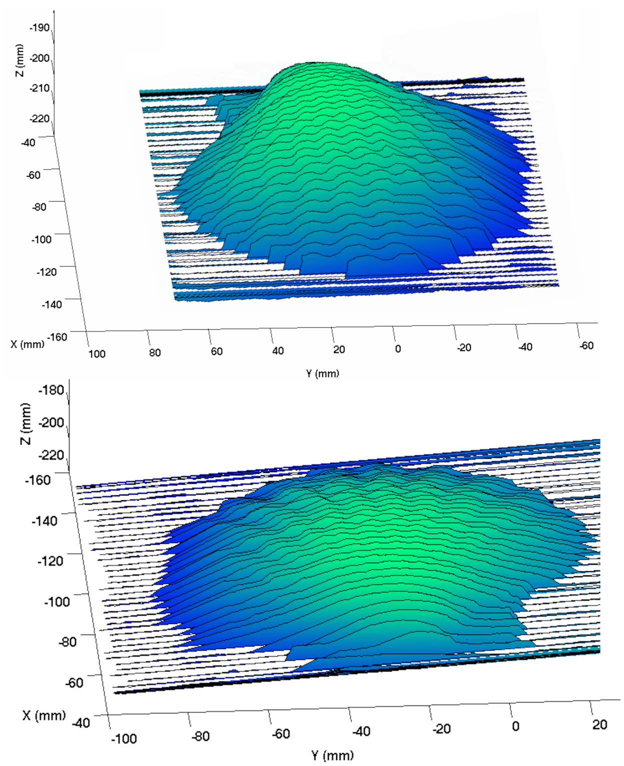


Fig. 7. 3D Scan Result

.

3D scan of scallop was conducted to display the 3D scan SLS capability, the results show about 2% error on the object size. In future work, we plan to use the SLS system for underwater inspection of ship hulls and harbor walls.

## Acknowledgments

This work is funded by the Portuguese government through FEDER funds Operational Programme for Competitiveness Factors of Incentives for Research and Technological Development System, Project No. 38907, and also by National Funds through the FCT (Portuguese Foundation for Science and Technology) within project Reference FCOMP-01-0124-FEDER-037281

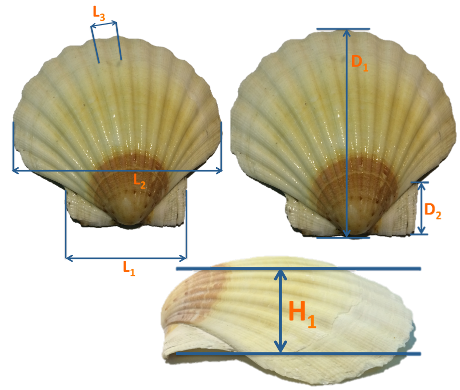


Fig. 8. Scallop measurements in different poses 0-2 left to right

.

## References

[1] Schechner, Y.Y.; Karpel, N., "Clear underwater vision," Computer Vision and Pattern Recognition, 2004. CVPR 2004. Proceedings of the 2004 IEEE Computer Society Conference on , vol.1, no., pp.I-536,I-543 Vol.1, 27 June-2 July 2004

[2] F. Bruno, G. Bianco, M. Muzzupappa, S. Barone, A.V. Razionale, "Experimentation of structured light and stereo vision for underwater 3D reconstruction", ISPRS Journal of Photogrammetry and Remote Sensing, Volume 66, Issue 4, July 2011, Pages 508-518, ISSN 0924-2716

[3] Srinivasa G., Narasimhan, S.K. Nayar, "Structured light methods for underwater imaging: light stripe scanning and photometric stereo," Proceedings of 2005 MTS/IEEE OCEANS, September, 2005, pp. 2610 - 2617.

[4] Inglis, G., Smart, C., Roman, C., Carey, S. "Detection of diffuse sea floor venting using structured light imaging". Poster OS11B-1473 presented at 2011 Fall Meeting, AGU, San Francisco, Calif., 5-9 Dec.

[5] C. Chen and A. Kak, "Modeling and calibration of a structured light scanner for 3-d robot vision," in IEEE International Conference on Robotics and Automation, vol. 4, 1987, pp. 807-815.

[6] D. Q. Huynh, R. A. Owens, and P. E. Hartmann, "Calibrating a structured light stripe system: A novel approach," International Journal of Computer Vision, vol. 33, pp. 73?86, 1999.

[7] Hartley, R., Zisserman, A.," Multiple View Geometry in Computer Vision" , Cambridge University Press , New York, NY, USA 2003.

[8] Yamauchi, K.; Saito, H.; Sato, Y., "Calibration of a structured light system by observing planar object from unknown viewpoints," 19th International Conference on Pattern Recognition ICPR 2008 , vol., no., pp.1,4, 8-11.

[9] Fuqiang Zhou, Guangjun Zhang, "Complete calibration of a structured light stripe vision sensor through planar target of unknown orientations", Image and Vision Computing, Volume 23, Issue 1, 1 January 2005, Pages 59-67, ISSN 0262-8856,

[10] Yang Yu, Zheng Bing, Zheng Hai-yong, Wang Zi-tao, Wu Guo-shuai and Wang Jin-cheng, "3D reconstruction for underwater laser line scanning," OCEANS - Bergen, 2013 MTS/IEEE , vol., no., pp.1,3, 10-14 June 2013, 10.1109/OCEANS-Bergen.2013.6607973

[11] C. Roman, G. Inglis, J. Rutter, "Application of structured light imaging for high resolution mapping of underwater archaeological sites," IEEE Oceans, Sydney, pp. 1-9, 2010.

[12] Zhang, Z., "Flexible Camera Calibration by Viewing a Plane from Unknown Orientations"., in International Conference on Computer Vision ICCV 2009, pp. 666-673.

[13] Harris, C., Stephens, M., "A Combined Corner and Edge Detector", in 'Proceedings of the 4th Alvey Vision Conference' , pp. 147–151, 1988.